Mat. Res. Soc. Symp. Proc. Vol. 685E © 2001 Materials Research Society

Ablation Lithography for TFT-LCD

Kenkichi Suzuki, Nobuaki Hayashi, Hiroshi Masuhara[1] and Thomas K. Lippert[2]
Displays, Hitachi, Ltd., 3300 Hayano, Mobara, Japan
[1]Applied Physics Department, Osaka University, Suita, Osaka, Japan
[2]Paul Scherrer Institut, CH-5232 Villigen PSI, Switzerland

ABSTRACT

Ablation lithography is based on the photo-decomposition ablation of polymer materials by excimer laser. It is a self-development process, and accordingly possible to reduce the throughput time and manufacturing cost of TFT-LCD. The major alterations from the conventional photolithography are the resist material and the mask. Developing both the technologies and using an experimental exposure& aligner, we fabricated a TFT pattern on 300 x 400 mm^2 glass substrate. The result proves the feasibility of EAL as an high throughput lithography suitable for a-Si TFT.

INTRODUCTION

The LCD (liquid crystal display) has been almost a synonym of FPD (flat panel displays), and the industry has been extended to the scale of nearly one tenth of that of semiconductor for recent 10 years. It is mainly due to a-Si TFT (thin film transistor)-LCD, which realized high display quality comparable to the conventional CRT, and the productions has increased concurrently with the enlargement of PC (personal computer) market. However there has been always discrepancy between the manufacturing cost and the price the market demands. The price has gone down regularly when the quantity increases (“crystal cycle”), and the manufacturers have coped with by reducing the cost and increasing sales by productions of larger sized and higher definition displays. Such circumstances are now changing, as rapid developments of information technologies demands variety of the displays, from small sizes for mobiles to larger sizes. Among them, especially large and high definition FPDs, e.g. more than 40” size, are very essential for expansion of FPD industry, because the new information system is fundamentally a combination of PC and TV. Although PC is still a large application field of TFT-LCD, it is very important to steer the development toward such displays, because they are actual drives to grow up the display market much more.

A question arises; is a-Si TFT-LCD competent to such displays with reasonable cost? Actually other displays, such as PDP (plasma display panel) and the low temperature p-Si (LTP)TFT, have started the productions. At present, PDP has a limitation in resolution and the cost reduction is not easy. LTP-TFT is most promising, especially its combination with organic EL, but its technical status is rather preliminary, far from low cost manufacturing meanwhile. On the other hand, a-Si TFT needs only slight improvements in the materials, processes, and designs to achieve the target performances. However, the production technology of a-Si TFT-LCD is almost matured, and the cost reduction is only achieved by reduction of the throughput time. The present throughput-up scheme is to use larger sized glass substrates, which resemble larger wafer in

LSI production. However there is essential difference in the size effect between TFT-LCD and LSI. In the latter case, larger wafer size constantly accompanies shrinkage of an effective chip size. However in the case of TFT-LCD, there is only enlargement of the "chip", and the larger substrate scheme is only effective for moderate sized displays (at most 15"), and not efficient for the larger sized LCD. Especially when we compare the equipments of the lithography and the depositions, the former now verges on the limit.

Accordingly we need improve the lithography process itself, and the present paper proposes a new method, excimer ablation lithography (EAL) which is feasible to improve the throughput time. The ablation (photo-decomposition ablation) is direct dissociation of atomic bonds by photons. The phenomenon was initially demonstrated by perforation of polymer materials by excimer laser irradiation [1,2]. It has been applied to machining of mainly micro holes, such as via holes in printed circuits boards [3] and ink jet nozzles. EAL is far more microscopic application of the ablation, and realizes self-development of resist [4,5]. The neglect of the development process is very effective to the manufacturing cost reduction. It eliminates a large foot print wet developing equipment, cleaning equipments, developer chemicals, and their disposal processes. In addition, the resist removal is a dry process, needless to use any vacuum system. The novel technologies proper to EAL are ablation resist and dielectric multiplayer mask. The following experimental details are devoted to the results of the investigations of these new technologies. In discussions, it is pointed out that the practical application of EAL is dependent upon the ablation rate of the resist polymers.

EXPERIMENTAL DETAILS

Figure 1 shows comparison between the conventional and ablation photolithography. In the latter case, the resist is irradiated by excimer laser through a mask, and the illuminated area is to be ablated. Thus it realizes self-development. Resist removal is done also by ablation. So EAL resist should be of photodecomposed type, different from the conventional one. The fluence on the substrate is nearly 100 mJ/cm^2 instead of conventional 20-30 mJ/cm^2. Due to the higher illumination intensity, alterations of the mask and the exposure & aligner are also necessary.

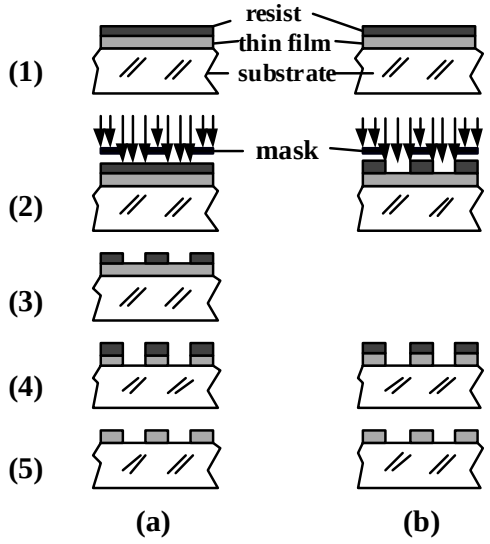

Figure 1. Comparison between conventional (a) and ablation (b) lithography. Sample is coated by resist (1), and exposed through a mask (2). The resist is developed (3), and after the film is etched (4), the resist is removed.

Ablation resist

As resist film is decomposesd during a short pulse period, the ejected fragments produce a shock wave, and they finally become a mushroom-shaped cloud called a plume. At the moment of ablation, a substrate is exerted by a mechanical stress due to momentum change [6], and a part of absorbed light is converted to heat. So as to prevent damages of the underneath thin films due to the effects, the resist should be ablated by as low fluence and as small shot number as possible. There is a window region in the fluence versus shot number relationship where outside of the lower limit no ablation occurs, and the higher limit is just threshold of the damage to the TFT films. Table Ⅰ shows the experimental results of the threshold values of the thin films constituent of a-Si TFT, which is defined as a fluence of appreciable damage after 20 shot irradiation. The threshold is higher when the films are covered by the resist than without. From the data, we decided 100 mJ/cm^2 as a working fluence, and looked for the materials with lower threshold fluence and less debris.

Table Ⅰ. Damage threshold of TFT films. Unit is mJ/cm^2.

Material	Film thickness (nm)	Direct	Resist covered
Cr	100	60	>150
Ta	150	75	>180
Al	200	150	>200
a-ITO	80	<50	>150
p-ITO	100	100	>150
SiN	300	100	>250
a-Si	200	120	>200

The KrF excimer laser (248 nm) is used, because it is in absorption band of aromatic ring [7], which is the most essential component of resist materials. Among various kinds of polymer materials, the thermoplastics were discarded, as they could not define any sharp edge by ablation. From the investigations of more than 100 thermosetting resins commercially available, we could observe two prominent features in the ablation phenomenon; a correlation between polymer molecular structure and ablation rate, and non-uniformity of the ablation rate over the illumination area even with uniform exposure.

A polymer structure consists of the main chains, the side chains, and the network. For a resist, it should include efficient light absorbers. There are two types of absorbing scheme of 248 nm, aromatic ring and doped chromophors. In our observations, the ablation rate is higher when the absorbance is larger. However, the light absorption by doped chromphors and the side chains are less efficient in ablation than by the main chains. There is a threshold of absorption coefficient, under which no ablation occurs. The value is about 10^4 cm^{-1} as shown in Figure 2. The rate larger than 0.02μm/shot is realized by such materials as, urethane, imide, novolac, melamin, and malain acid. It is notable that the ablation rate is almost same to the same kind of polymer, and it suggests the ablation rate is inherent to the main chain structure. Among them, the highest rate is found both in polyurethane (PU) [8] and polyimide (PI), and we concentrated to two materials, aiming to improve the ablation rate by changing the molecular structures.The fundamental structure of PI is shown in Figure 3. We synthesized 27 samples, combinations of various R_1 (acid anhydride) and R_2 (diamine). The result is that there is no appreciable improvement in the ablation rate, and that particle size of debris is not reduced. There is no correlation between the structures and the ablation rates. The result reinforces the

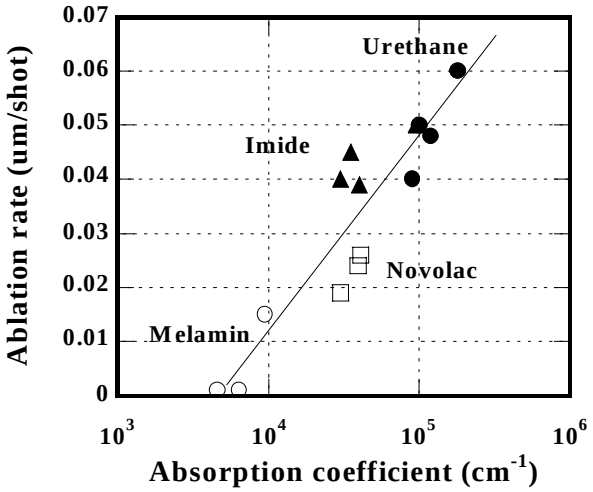

Figure 2. Relationship between ablation rate and absorption coefficient.

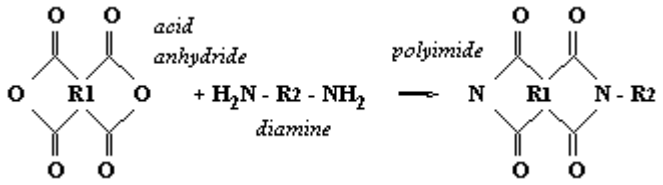

Figure 3. Fundamental structure of polyimide.

observation that the rate is only dependent upon a characteristic structure of the polymer. It is inferred that the dissociation may occur at a certain bond location photochemically, but the rigid networks characteristic to PU produce comparatively large sized particles.

Polyurethane is a polymer including some amounts of urethane bonds, which is polymerized by reactions of diisocyanate and diol as shown in Figure 4. There are more than ten isocyanate main chain (denoted by R) and very many polyols (R'). For our application, we adopted 3 kinds of isocyanate (TDI, MDI, and HDI) and various polyols. We synthesized approximately 70 combinations of those main chains and variations of the side chains and networks. All the samples showed almost gaseous products at ablation. From the rate measurements, we could deduce the following results; 1) HDI is not effective in absorption and dissociation, 2) TDI is better than MDI, 3) The effect of dissociation of nitro benzyl alcohol is near one half of direct bond of N to MDI, 4) The shorter polyol bond is better for dissociation, 5) Chain structure is better than ring [9]. In

Figure 4. Fundamental structure of polyurethane. Table shows 3 kinds of isocyanate.

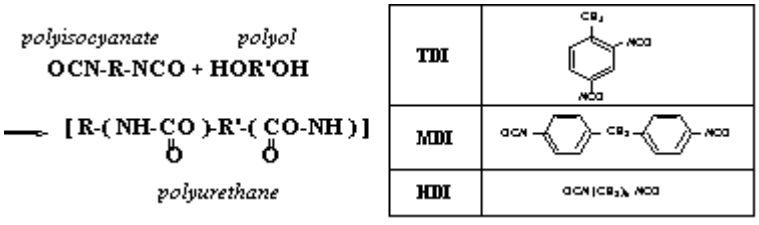

spite of the extensive investigations, we could obtain only slight improvement of the ablation rate. This also seems to prove that ablation rate is inherent to the main chain structure. We selected a standard ablation resist among the polyurethane polymers, taking into considerations of durability to various TFT etchants and dry etching environments. The ablation rate is 0.06μm/shot.

Ablation rates were measured for 1 mm^2 square illumination area. It was found the ablation rate is larger at the edge than at the centre as shown in Figure 5. The feature is observed for all the patterns, circle, triangle and rectangular. The rate at the edge is not much different among relatively higher rate polymers, and the difference in the rate is mainly attributed to the rate at the centre. The behaviour is related to the ablation dynamics, and we observed plume dynamics by the shadowgraphy [10]. Typical pictures of novolac type resist OFPR 800 are shown in Figure 6. At the delay time less than 1μs, a uniform rise of "fluid" is observed, which produces shock wave front in the atmosphere. The front is extinguished after 10μs, and then the fluid expands and after several ten μs a mashroom shape cloud is formed, which resembles atomic bomb cloud. The details are different among materials and the atmosphere, however the general features are almost same.

Figure 5. Difference of ablation depth by sites and materials((a) polyurethane and (b) novolac).

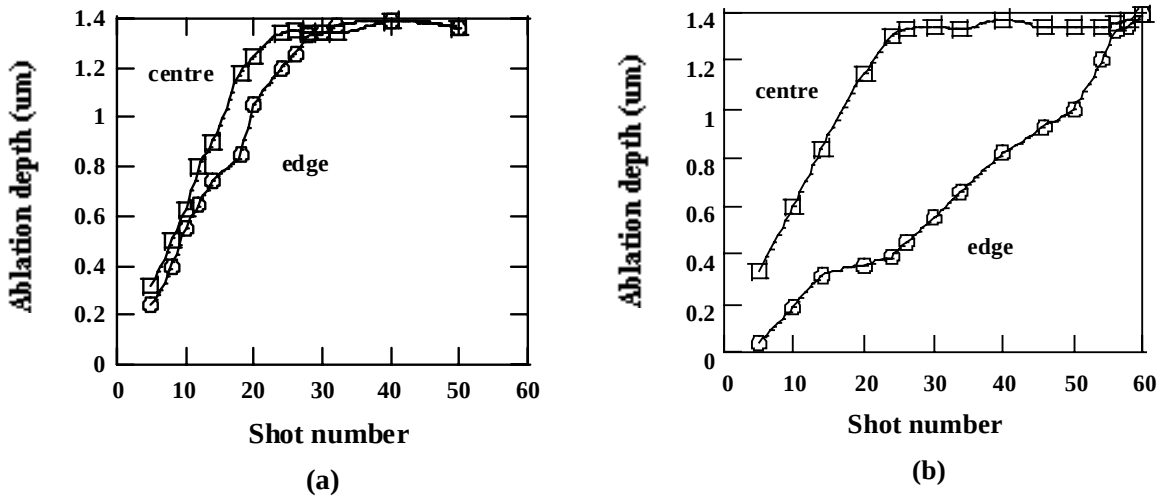

Figure 6. Shadowgraphy pictures of polymer ablation after delay time of 1 μs (a), 8 μs, and 80 μs.

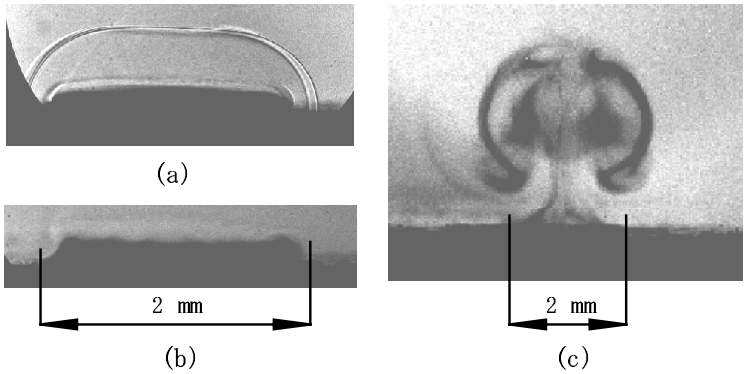

The difference of the ablation rate at the edge and at the centre may be related to formation of debris. If debris include much large sized particles, some would remain at the centre of the illumination area. We measured the profiles of the ablated holes shot by shot. The remaining debris at the centre might act as a light shield and reduce the rate. In the case of polyurethane which produce only gaseous products, the rate difference by sites is not so large.

Dielectric multilayer mask

The fluence 100 mJ/cm^2 on the surface of the sample means nearly 200 mJ/cm^2 on the mask. The damage level of Cr layer is less than 60 mJ/cm^2 and we used a dielectric multilayer reflector film as an alternative of Cr. The film consists of stratified periodic layers of SiO_2 and HfO_2 of 1/4 wavelength optical thickness [11]. One layer thickness of HfO_2 is 27 μm, and that of SiO_2 is 43 μm for 248 nm. The films are deposited by vacuum evaporation. The mask patterns are fabricated using ion milling and dry etching processes in which Cr is used for resist. For the evaluation of the mask, we made a conventional test patterns, where the minimum line and space is 1.5 μm. The angle of the side wall to the substrate surface is 69 °.

The reflectivity of the dielectric multilayer is 0.99 for 6 period [12]. It may be enough for mask, but the total thickness is 420 nm. For practical applications, it is indispensable to repair defects in the mask. The simplest method is double deposition, and it results double thickness. So it is essential to elucidate the influence of the thickness to the image formation. Figure 7 shows the configuration of the simulation where a mask is represented by 2 μm width slit with infinite length. So it is 2-dimensional calculation. The diffraction pattern of just behind the mask is calculated by FD-TDM (finite difference-time domain method), which solves time dependent Maxwell equation precisely for any medium. In Figure 8(a), Fresnel diffraction patterns at 2 wavelengths behind the mask are shown. The Fresnel pattern is Fourier-transformed, and among the constitutive plane waves, those of which k-vector is within angle corresponding to N.A. are selected to make image. The procedure is just inverse Fourier transform by a imaging lens. Figure 8(b) shows examples of the image for the x 3 lens with N.A.=0.1 for three thickness of layer. The zero thickness corresponds to Cr mask. According to the calculation as to various N.A., it is concluded that 12 layer mask is almost same to Cr masks up to N.A.= 0.2. As the N.A. of the mirror projection type aligner is limited to 0.135, the dielectric multiplayer mask is usable for a-Si TFT. The resolution of the resist patterns was measured using the optics stated below and the test pattern masks. We could obtain very clear 2 μm line & space resolution.

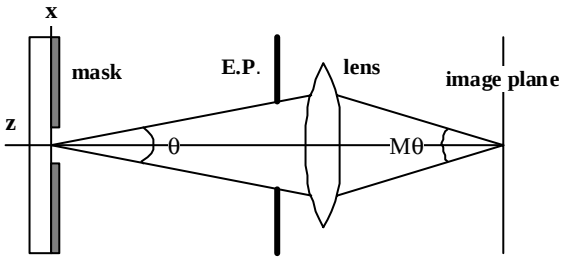

Figure 7. Configuration of image forming simulation by dielectric multilayer mask. The mask is represented by 2 μm width slit of infinite length. The mask is illuminated uniformly. N. A. =nsin θ . M is magnification of the lens.

Figure 8. Examples of the simulation; (a) diffraction pattern just behind the mask, and (b) image for three kinds of mask by x 3 imaging lens.

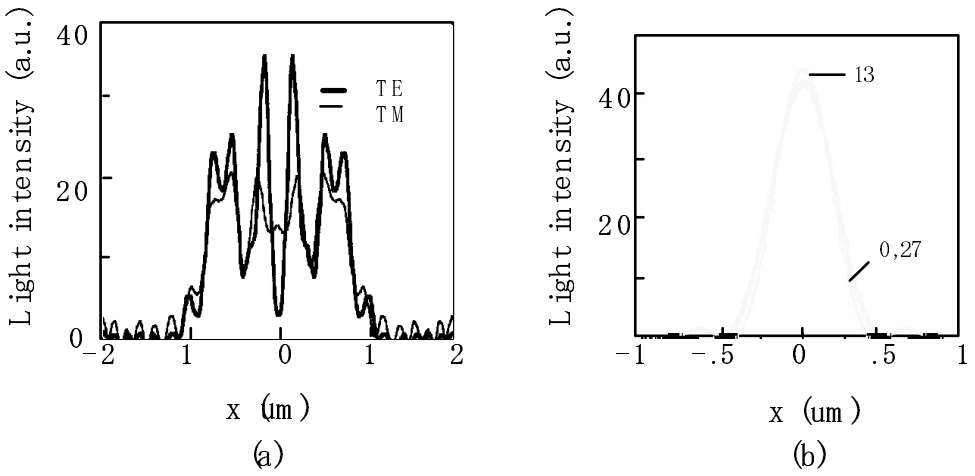

Experiments

The aim of the experiments is to verify the precision of the TFT film patterns processed by EAL and especially exposed by step & scan system for an actual sized substrate. For this purpose, we fabricated "ablation aligner". The structure is very similar to the conventional LSI aligner-exposure. The light source is an excimer laser Lambda Physik LPX 210i (KrF 670 mJ output, max. 100 Hz repetition rate, and 30 ns pulse width). The optics consists of an attenuator, a homogenizer & beam shaper to make a 2 x 45 mm^2 uniform mask illumination. The N.A. of the imaging lens is 0.1, and 1:1 telecentric and symmetrical refractive type. The length is 511 mm, and the effective diameter is 55 mm. The working distance of the lens is 70mm. It is placed between two sets of X-Y stages, one for a mask and the other for a substrate. Both the stages (Aerotech Unidex 30) scan 300mm x 300mm area. In spite of the scanning area, we used. 300 x 400 mm^2 glass substrate, with an auxiliary jig. The mask patterns over the illumination area are projected one to one on the substrate through the imaging lens. The step & scan system does not need whole pattern. The pattern is A4 sized BM (Black matrix), which consists of lattice with line width of 24 μm and with the pitch of 88 x 264 μm. The lattice of the BM pattern is divided into 5 equal parts, of which width is just covered by illumination area. A dielectric multilayer mask was fabricated on 8"x 8" quartz substrate, consisting of the part of the lattice and 4 unrepeated patterns. For one pattern, both the stages move antiparallely, and then the mask stage moves stepwise perpendicular to the scanning direction corresponding to other pattern. The whole patterning is completed by repetition of the motions.

In the experiment, we chose sputtered Cr as a BM film. The film thickness is 110 nm. The ablation resist polymer is a polyurethane, of which ablation rate is 0.06 μm/shot at 100 mJ/cm^2. The ablation resist was spin-coated and the thickness was 1μm. The shot number /site is 20. The scan speed is 5 mm/s. One scan spans 200mm, and it takes 40 seconds. We needed 7 scans to cover one A4 BM area, and thus it took 287 seconds including 7 stepwise motions. During ablation the plume was sucked by vacuum cleaner. The gas speed at the sucking nozzle point was about 20m/s in the atmosphere, and the debris is eliminated completely.

After

Figure 9. Comparison of the patterns of (a) dielectric multilayer mask, (b) ablated resist, and etched Cr.

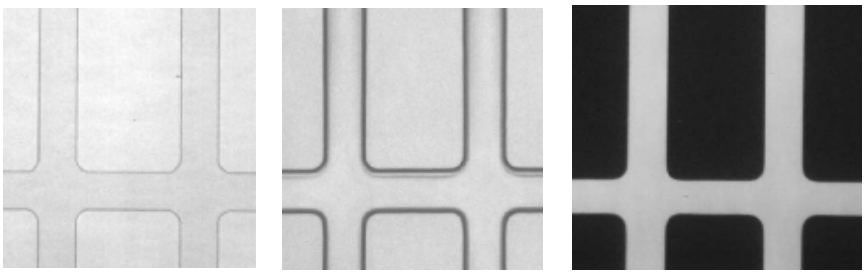

(a) (b) (c)

ablation, the substrate was O_2-ashed, and Cr was etched by Cr etchant (water solution of $Ce(NH_4)_2(NO_3)_6$ and $HClO_4$). The remaining resist was removed by ablation, and again O_2-ashed. Figure 9 shows optical micrographs of a part of the dielectric mask, a resist pattern, and a etched Cr pattern. It was rather difficult to detect pattern size difference by the local pattern. We compared whole patterns of the mask and the etched substrate by a telecomparator. The difference in the long side(218 mm) is 3μm, and that of the short side(163mm) is 12μm. As scanning is along the short side, the large discrepancy is due to difference in speed of both the stages. Considering the mechanical structure of our experimental setup, the precision is reasonable, and it verifies the feasibility of the step & scan system for EAL process.

DISCUSSIONS

The resultant throughput time by the experimental equipment is far longer than that of up-to-date production lines of a-Si TFT. The most advanced production lines at present use 920 x 730 mm^2 substrate, and the throughput time of the lithography is 60 seconds, where exposure time is 50 and mechanical time is 10 seconds. Table Ⅱ shows the factors determining throughput time of EAL. Possible figures are assigned to these factors for three cases. Here the most essential improvement is output power of the excimer laser. The high power excimer laser source is being developed mainly for applications to excimer laser crystallization for LTP-TFT, and 1J output and 250 Hz repetition rate is now available. Besides a laser manufacturer announces the production of a higher output laser, 4J output and 250 Hz repetition rate in near future. The N.A. of the image lens is assumed to be 0.1 in all cases. The value is reasonable to a-Si TFT application. The item "state-of –art " means the same technical level to the present experiment, but it is assumed a

Table Ⅱ. Estimation of throughput time.

	State-of-art	First target	Second target
Shot number /site	20	20	20
Laser output (mJ)	670	1000	4000
Power loss (%)	50	40	35
Power at image (mJ)	300	600	2600
Lens diameter (mm dia)	70	120	20 x 260
Mask illumination area (mm^2)	5 x 60	6 x 100	10 x 260
Laser repetition frequency (Hz)	250	250	250
Ablation time (sec)	187	98	22

manufacturing machinery. For the first target, we adopt the 1J excimer laser and a little larger lens (120 mm diameter refractive type). The size of the lens is actually used for stepper for a-Si TFT. The working time, 98 sec, for ablation is two tomes of that of the mass production. In the second target, the exposure & aligner is assumed to be a mirror projection type similar to the present manufacturing machine, in which the illumination size is 14 x 260 mm^2. The throughput time is 22 seconds. This is just one half of the present manufacturing scheme. However for practical application, we have to take into considerations of various kinds of new technologies such as the dielectric multilayer mask (including repair), reflection coating of the optical components of the mirror projector, and O_2 ashing. Although these are not so vital problems, more drastic improvement is necessary to motivate to replace the conventional method with EAL The possibility is relied only on improvement of the ablation rate of the resist. Actually if we can get one half of the rate, the first target is just same throughput time to the present scheme, and due to simple imaging lens, the machine cost will be much reduced.

In so far as our investigations, there is a limitation in the ablation rate inherent to the main chain structures. Among them we found the most efficient materials are PU and PI. It is notable that the both polymer have a same main chain structure, an aromatic ring with directly connected to N (phenyl carbamate). Among so many polymers it is only one structure with an appreciable ablation rate at 100 mJ/cm^2 . In such fluence region, the ablation depth is proportional to absorption coefficient as stated previously. This is completely different from the empirical formula for the ordinary ablation. The established ablation model is that the absorbed light is converted to thermal vibration of local structures (a hot spot) and the motion scissors molecular bonds [13]. Thus it is a thermal process. The threshold fluence is one or two order higher than that of the present cases. Accordingly the higher rate of conventional ablation is due to multiphoton process, and so at low fluence as 100 mJ/cm^2, ablation mechanism is infered to be a genuine photodecomposition process, as the participated photon is only small number (less than 1 photon per a dissociation unit) to excite thermal vibrations.

Our observations show only slight numbers of the bond structures are effective to dissociation at low photon number, and the unit in the bonds should be proximate to the absorption centres. In the thermal ablation, doped chromophors are very efficient sensitizer, and enhance the ablation rate[14]. However it is not so in the present case. This means efficiency of photodecomposition is closely related to energy transfer to the effective dissociation units. In the result, our investigation was to find the most effective photodecomposition unit which correlates with aromatic rings. This may be a reason why we found only a single material among so many industrial polymers. Another interesting feature is the role of the side chains and network structures. Contrary to the subtle photodecomposition mechanism, the effects are understandable by somehow simple mechanical model. The effect is clearly revealed in the many respects, such as differences between thermoplastics and thermosettings, differences between PI and PU, and differences among PU.

Although it seems to be a rare material that can realize higher ablation rate at low fluence, a new type of polymer have been proposed recently, which is characterized by photolabile group (-N=N-N-X-) [15]. The absorption maximum can be tailored for 308 or 351 nm. Many kinds of the derivatives show higher ablation rate (0.15um/shot at 100mJ/cm2), and in addition, they only produce gaseous products including nitrogen.

The experiments of TOF-MS show that the decomposition is completely photochemical. The durability to etchants are now under examination, and preliminary results show it is durable for the etchants for Al and ITO. A problem of the materials is that it is a little difficult to spin-coat. Solving such a practical problem and elucidating the direct photodecomposition mechanisms would lead to innovations of display industry.

REFERNECES

1. Y. Kawamura, K. Toyoda, and S. Namba, Appl. Phys. Lett. **40**, 374 (1982)
2. R. Srinivasan, V. Mayne-Banton, Appl. Phys. Lett. **41**, 578 (1982)
3. R. S. Patel, T. F. Redmond, C. Tessler, D. Tudryn, and D. Pulaski, Intn'l J. Microcircuit and Electronic Packaging **18**, 266 (1995)
4. G.M.Davis, A.F.Gibson, M.C.Gower, R.A. Lawes and R.A.Moody, in Microcircuit Engineering '83 (Cambridge, 1983)
5. K. Suzuki, M. Matsuda, T. Ogino, N. Hayashi, T. Terabayashi, and K. Amemiya, Proc. SPIE **2992**, 98 (1997)
6. M. A. Shannon and R. E. Russo, Appl. Phys. Lett. **67**, 3227 (1995)
7. L. Lang, Absorption spectra in the ultraviolet and visible region, (Publishing House of Hungarian Academy of Science, Budapest, 1964) vol.**2**
8. S. Kueper and J. Brannon, Proc. SPIE **1598**, 27 (1991)
9. S. M. W. Bennett, The synthesis and UV-laser ablation of polyurethane, Thesis, University of Hull (1995)
10. R. Srinivasan, K. G. Casey, and B. Braren, Chemtronics **4**, 153 (1989)
11. F. Rainer, W. H. Lowdermilk, D. Milam, C. K. Carniglia, T. T. Hart, and T. L. Lichtenstein, Appl. Opt. **24**, 496 (1985)
12. M. Born and E. Wolf, Principle of optics, (Pergamon Press, 4th ed. 1970) pp.51-70
13. H. Fukumura, N. Mibuka, S. Eura, H. Masuhara, and N. Nishi, J. Phys. Chem.**97**, 13761 (1993)
14. T. Lippert, A. Yabe, and A. Wokaun, Adv. Mater. **9**, 105 (1997)
15. T. Lippert, L. S. Bennett, T. Kunz, C. Hahn, A. Wokaun, H. Furutani, H. Fukumura, H. Masuhara, T. Nakamura, and A. Yabe, Proc. SPIE **2992**, 135 (1997)